Morphology of spinodal decomposition

Klaus R. Mecke[1] and Victor Sofonea[1,2]

[1]*Fachbereich Physik, Bergische Universität Wuppertal, D-42097 Wuppertal, Federal Republic of Germany*

[2]*Research Center for Hydrodynamics, Cavitation and Magnetic Fluids, ''Politehnica'' University of Timişoara, Mihai Viteazul 1, R-1900 Timişoara, Romania*

(Received 15 May 1997)

The morphology of homogeneous phases during spinodal decomposition, i.e., the scaling of the content, shape, and connectivity of spatial structures is described by a family of morphological measures, known as Minkowski functionals. Besides providing means to determine the characteristic length scale L in a statistically robust and computationally inexpensive way, the measures allow also one to define the crossover from the early stage decomposition to the late stage domain growth. We observe the scaling behavior $L\sim t^{\alpha}$ with $\alpha=1/3$, $\alpha=1/2$, and $\alpha=2/3$ depending on the viscosity. When approaching the spinodal ρ_{sp}, we recover the prediction $L\sim(\rho-\rho_{sp})^{-1/2}$ for the early time decomposition.
[S1063-651X(97)51609-6]

PACS number(s): 47.20.Hw, 64.60.Qb, 05.70.Ln, 02.70.Ns

The morphological characterization of patterns becomes more and more important in statistical physics since complex spatial structures emerge nowadays in many physical systems. Phase separation kinetics is probably the most convenient way to generate irregular spatial patterns on a mesoscopic scale. Such patterns arise after a sudden quench of the homogeneous fluid into the two-phase coexistence region where the fluid separates into the coexisting liquid and vapor phases [1]. A particular effort in recent years was focused on the evidentiation of different scaling regimes via appropriate computer simulations, in particular molecular dynamics [2,3], Ginzburg-Landau models [4], lattice gas [5], lattice Boltzmann [6–8], and dissipative particle dynamics [9].

The usual approach to determine the time dependent mean domain size $L(t)$ is using the first zero or the first moment of the radial distribution function. Besides being computationally expensive and exhibiting large fluctuations in small systems, the mean domain size alone cannot account for the morphology of the rich variety of geometrical shapes of domains. Therefore, it is useful to look for a quantitative characterization of the morphology, i.e., of the time evolution of content, shape, and connectivity of spatial patterns. The aim of this paper is to point out that integral geometry [10,11] supplies a suitable family of such topological as well as geometrical descriptors which are well known as *Minkowski functionals* in digital picture analysis and mathematical morphology [12]. In a d-dimensional ambient space the number of these functionals is $d+1$. In the two-dimensional case the three Minkowski functionals are related to familiar measures: covered area, boundary length, and Euler characteristic (connectivity).

Nearly every continuous pattern can be decomposed in black and white convex subsets using a thresholding procedure [13]. For instance, one has often an underlying pixel structure due to the finite resolution of the experimental equipment or to the inherent discrete nature of computer simulations performed on a lattice. Each pixel, e.g., squares or hexagons in two dimensions, is a compact, convex set and the whole pattern is the union of all of these pixels. So let us consider a homogeneous domain $A=\cup_i K_i\subset\mathbb{R}^d$, which can be represented as a finite union of compact convex sets K_i, for instance hexagons. Let $\mathcal{R}$ denote the class of such subsets of $\mathbb{R}^d$. Morphological measures are defined as functionals $\mathcal{W}$: $\mathcal{R}\to\mathbb{R}$ on homogeneous domains, i.e., on subsets $A\in\mathcal{R}$ of $\mathbb{R}^d$. Let us now define three general properties a functional should possess in order to be a morphological measure:

(i) *Additivity.* The functional of the union $A\cup B$ of two domains equals the sum of the functional of the single domains subtracted by their intersection

$$\mathcal{W}(A\cup B)=\mathcal{W}(A)+\mathcal{W}(B)-\mathcal{W}(A\cap B). \tag{1}$$

This relation generalizes the common rule for the sum of the volume of two domains.

(ii) *Motion invariance.* The morphological measure of a domain A is independent of its location and orientation in space, i.e., $\mathcal{W}(gA)=\mathcal{W}(A)$, where gA denotes the translated or rotated domain.

(iii) *Continuity.* If a sequence of convex sets K_n converges towards the convex set K for $n\to\infty$, then $\mathcal{W}(K_n)\to\mathcal{W}(K)$. Intuitively, this property expresses the fact that an approximation of a convex domain K by convex polyhedra K_n, for example, also yields an approximation of $\mathcal{W}(K)$ by $\mathcal{W}(K_n)$.

Obviously, the area F and the boundary length U of a domain obey the three conditions (i)–(iii). Another continuous, motion invariant and additive quantity is the Euler characteristics $\chi:=N^w-N^b$, which is defined in two dimensions as the difference between the number of connected domains N^w (white) and the number of uncovered holes N^b (black).

A remarkable theorem in integral geometry is the completeness of the morphological measures [11] which asserts that any additive, motion invariant and conditional continuous functional $\mathcal{W}(A)$ defined on subsets $A\in\mathcal{R}$, is a linear combination of the $d+1$ Minkowski functionals, $\mathcal{W}(A)=\sum_{\nu=0}^{d}c_\nu W_\nu(A)$ with real coefficients c_ν independent of A. In other words, the Minkowski functionals are the complete set of morphological measures defined by the properties (i)–(iii). In $d=2$ the Minkowski functionals are related to familiar measures, the covered area $F=W_0$, the boundary length $U=2W_1$, and the Euler characteristic $\chi=W_2/\pi$. We em-

phasize that the Minkowski functional W_ν is homogeneous of order $d-\nu$, i.e, for a dilated domain λA one obtains

$$W_\nu(\lambda A)=\lambda^{d-\nu}W_\nu(A)\,. \tag{2}$$

These relations enable one to define a time-dependent scaling length by the morphological measures. Because of the properties (i)–(iii) and of the scaling relation (2), we expect the Minkowski functionals to be suitable measures to characterize the morphology of patterns in a consistent way.

In order to get detailed information about the spatial structure of the spinodal decomposition, we adopted the modeling of the isothermal hydrodynamics achieved in Refs. [7,8] as a lattice Boltzmann model on a 2D hexagonal lattice with unit vectors $\vec{e}_i$, $i=0,\ldots,6$. The particle distribution functions $f_i(\vec{x},t)$ evolve in accordance to the discretized Boltzmann equation $f_i(\vec{x}+\vec{e}_i,t+1)-f_i(\vec{x},t)=\Omega_i(\vec{x},t)$ with the linearized collision term $\Omega_i(\vec{x},t)=-(f_i-f_i^{eq})/\tau$ introducing the equilibrium distribution functions f_i^{eq}, as well as the relaxation time $\tau>1/2$. In order to have a Van der Waals fluid, the bulk free energy density ψ has the form $\psi=-\rho T\,\ln(1/\rho-b)-a\rho^2$, where T is the system temperature and $\rho(\vec{x},t)=\Sigma_i f_i(\vec{x},t)$ the local particle density. Additionally, a surface tension κ is introduced accounting for energy contributions due to inhomogeneous densities $\rho(\vec{x})$. Choosing $a=9/49$, $b=2/21$, the critical temperature value becomes $T_c=0.571$. The spinodal densities $\rho_{sp}^{\pm}$ at temperature $T<T_c$ are defined as the zeros of the equation $\psi''(\rho)=0$. For $T=0.550$, one obtains the densities $\rho_{sp}^{-}=2.744$ and $\rho_{sp}^{+}=4.315$.

Our subsequent simulations were mainly done on lattices with 1024×1024 nodes using periodic boundary conditions. Each simulation run was defined by the value of the mean density ρ, and the value of the relaxation time τ. Most simulations were done with the value $\kappa=0.01$ of the surface tension constant, which ensures the width of the interface region between homogeneous phases to be approximately five lattice units. The lattice system was first initialized with a mean density ρ and 1% random fluctuations of the local density $\rho(\vec{x})$ were allowed around the mean value. After each initialization the system was released to evolve during 500 preliminary automaton steps at the initial temperature $T_{in}=0.580$ above the critical one, then the temperature was suddenly changed to the final value $T_{fin}=0.550$. Starting from this moment $(t=0)$, the system was allowed to evolve to its equilibrium state while the patterns were characterized through the values of the Minkowski functionals. A threshold density ρ_{th} is introduced and the gray value at each pixel is set to either white or black depending on whether the original local density value $\rho(\vec{x})$ is larger or lower than ρ_{th}, respectively. Because no significant threshold dependence of the Minkowski functionals is observed after $t\approx200$, the threshold will be set further to the medium density value $\rho_{th}=3.5$.

The first obvious quantity describing the morphological differences in digital images is the relative white area, $F:=N_{\rho_{th}}/N$, i.e., the number $N_{\rho_{th}}$ of the pixels in the original image having the corresponding gray level $\rho(\vec{x})$ greater than ρ_{th}, normalized by the total number N of pixels. The

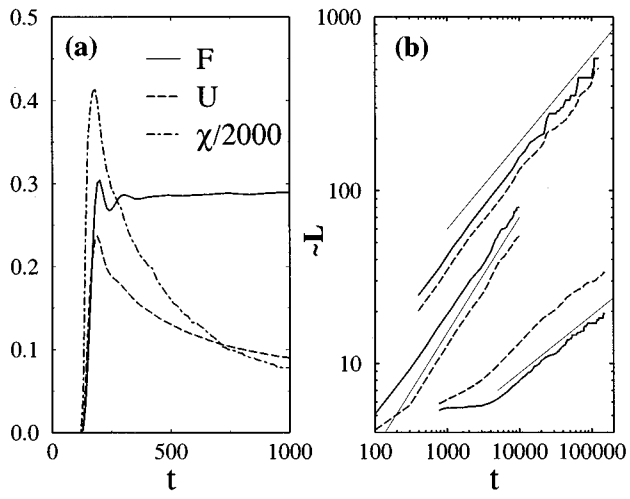

FIG. 1. (a) Time evolution of the morphological measures F, U, and χ at the mean density $\rho=3.0$ and the parameters $\kappa=0.01$, $\tau=0.60$. (b) The boundary length $w_1/U(t)$ (dashed line), and the connectivity $w_2/\chi(t)^{-1/2}$ (thick solid line) show the scaling relation (3) with the exponents $\alpha=2/3$ ($\tau=0.53$, $w_1=1$, $w_2=400$), $\alpha=1/2$ ($\tau=0.6$, $w_1=0.5$, $w_2=1000$), and $\alpha=1/3$ ($\tau=1.5$, $w_1=0.5$, $w_2=80$) indicated by thin solid lines. The coefficients w_i are chosen to separate the data.

second morphological quantity is $U:=B/N$ defined as the ratio between the total length B of the boundary lines separating black and white regions, normalized by the total number of pixels. To determine B one has to count the numbers of pairs of neighbored black and white pixels.

The third quantity of interest, the Euler characteristics $\chi=N^w-N^b$, defined by the difference of the number of connected components, is not normalized by the total number of pixels in order to keep integer numbers. This quantity describes the connectivity of the domains in the lattice and, e.g., it equals -1 when one has a black drop in a large white lattice and $+1$ vice versa. The ratio $\chi/(UN)$ describes the mean curvature of the boundary line separating black and white domains. Despite its global meaning, the Euler characteristics may be calculated in a local way using the additivity relation (1) as already suggested in the case of a square lattice [13]. Thus the three morphological measures F, U, and χ can be simply determined from pixel counting operations, i.e., using a very fast and convenient method.

In Fig. 1(a) we show the time dependence of the morphological measures $F(t)$, $U(t)$, and $\chi(t)$ for an off-symmetric quench, $\rho=3.0$, where the fluid phase is the minority phase. One can clearly distinguish two different time regimes: the early stage of spinodal decomposition kinetics and the late stage of domain growth. At early times, the growth of density fluctuations leads to the build up of interfaces between homogeneous domains of the two coexisting phases. This process is accompanied by an increase of the white area F belonging to the liquid phase, as well as of the boundary length U of the interface. Also the Euler characteristic increases, because many disconnected components of the minority phase arise. In contrast to this early stage, the late stage domain growth is characterized by a decrease of the quantities U and χ, which is a direct consequence of the increase of the characteristic length scale. The area of the

liquid phase remains quite constant and approaches the final value $F(t\to\infty)\to(\rho-\rho_{gas})/(\rho_{liquid}-\rho_{gas})$, which is given by the level rule of the coexistence region. The oscillations of $F(t)$ in Fig. 1(a) indicate shape fluctuations of the domains due to the redistribution of particles in the interface region, which are less favored at higher fluid viscosities. They are driven by the surface tension and the inertia of the fluid which compete at the crossover from spinodal decomposition to domain growth. Because of phase demixing, the boundary length U and the Euler characteristic approach their final minimum values $U(t\to\infty)\to 8\sqrt{F/\pi N}$ and $\chi(t\to\infty)\to 1$, which correspond to a single liquid drop of area F, immersed into the vapor phase.

The magnitudes of $U(t)$ and $\chi(t)$ increase during the early stage due to the formation of homogeneous domains, i.e., of sharp boundaries separating the phases. After domains have been formed, the boundary length $U(t)$ as well as the connectivity $\chi(t)$ decrease due to the growth of the domains. Their maximum values $\overline{U}$ and $\overline{\chi}$ mark the transition point, i.e., the crossover from the phase development during spinodal decomposition and the domain growth. Consequently, their positions $t_{max}(U)$ and $t_{max}(\chi)$ may be used to define the transition (crossover) time $\overline{t}$ which marks the onset of domain growth and the end of the spinodal decomposition. Although the values generally differ slightly, the difference is quantitatively not relevant and both times mark the same transition in the time evolution. We will conventionally use the maximum of the boundary length U to define the transition time, i.e., $\overline{t}:=t_{max}(U)$. The crossover time $\overline{t}$ from spinodal decomposition to domain growth does not depend on the surface tension κ but it has a linear dependence on the relaxation time τ. After the crossover time the volume $F(t)$ has approached the final value and we can consider this value as constant despite the decaying oscillations. If the inhomogeneous pattern consists of homogeneous domains with sharp interfaces, i.e., if well-defined domains exist, the domain growth process is achieved via the rearranging of domains without changing the relative area F of the liquid phase which is given by the level rule. Because the measures $W_\nu(A)$ are homogeneous functions of order $d-\nu$ [see Eq. (2)], we assume the following scaling behavior of the Minkowski functionals:

$$F\sim 1, \quad U\sim L^{-1}, \quad \chi\sim L^{-2}, \tag{3}$$

with the scaling length L. We have tested this assumption concerning the scaling behavior of the morphology by changing system parameters as surface tension κ and relaxation time τ, and looking for the same functional behavior of U^2 and χ. Thus, it is possible to define the characteristic length $L(t)$ starting either from the Euler-characteristic $L_\chi(t):=\chi(t)^{-1/2}$ or from the boundary length $L_U(t):=U(t)^{-1}$.

There are other possibilities to define length scales of spatial patterns such as the first zero of the correlation function or the first moment of the wavelength distribution. These definitions, although widely used by many authors, are recognized to be computationally expensive [3]. The definition (3) of the length L allows a faster computation algorithm, because it does not involve Fourier transformations but only pixel counting, and has also a direct geometric interpretation. Therefore, we are able to look for the scaling of the morphology.

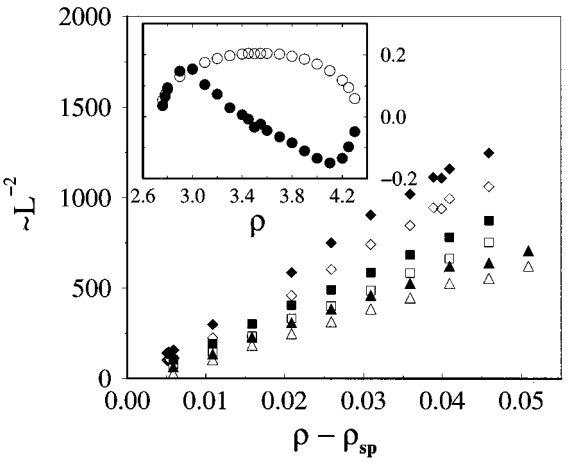

FIG. 2. Dependence of the Euler-characteristic $\chi(\overline{t})/2000$ (filled symbols) and the boundary length $U(\overline{t})$ (open symbols) at the onset of growth on the mean density ρ (spinodal density is $\rho_{sp}^{-}=2.744$ at $T=0.55$, $\tau=0.8$). The length scale $L(\overline{t})\sim(\rho-\rho_{sp}^{-})^{-1/2}$ diverges at the onset of the domain growth $\overline{t}$ [$\tau=0.6$ (diamonds), $\tau=0.7$ (squares), and $\tau=0.8$ (triangles)]. It can be measured either by $\chi(\overline{t})^{-1/2}$ or by $U(\overline{t})^{-1}$.

The possibility to distinguish between the early time spinodal decomposition and the late stage domain growth, which are delimited by the transition time $\overline{t}$, allows us to study the scaling length $\overline{L}(\rho):=L(\overline{t})$ at the onset of growth $\overline{t}$, i.e., at the end of the decomposition regime. The length $\overline{L}$ does not depend significantly on the surface tension κ but it depends linearly on τ. Thus κ has an influence on the shape of the domains, but it has no singnificant influence on the length scale. The inset of Fig. 2 shows the dependence of the morphology, i.e., the Euler characteristic $\overline{\chi}:=\chi(\overline{t})$ and the boundary length $\overline{U}:=U(\overline{t})$ of the patterns on the mean density ρ at the onset $\overline{t}$ of growth. One observes a parabolic behavior of $\overline{U}(\rho)$, which reaches its maximum for $\rho=3.5$, i.e., for bicontinuous patterns. The Euler characteristic $\overline{\chi}(\rho)$, i.e., the mean curvature is positive as long as the high density phase (white domains) is the minority phase forming many droplets within a sea of low density phase for $\rho<3.5$. It becomes negative in the opposite case, and it is zero for the symmetric decomposition indicating a vanishing mean curvature of the boundary lines. Approaching the spinodal density $\rho_{sp}^{-}=2.744$ at $T=0.550$ we observe the relation $\overline{L}(\rho\to\rho_{sp})\sim(\rho-\rho_{sp}^{-})^{-1/2}$ for the characteristic length scale of spinodal decompositon (Fig. 2). The scaling is consistent with the prediction of the Cahn-Hilliard theory of early time spinodal decomposition [1]. For the onset time $\overline{t}$ we observe the analogous relation $\overline{t}(\rho)\sim\overline{L}(\rho)$, indicating a density independent mean velocity $\overline{L}/\overline{t}$ of the fluid particles during the early stage, which depends only on the temperature T. Cahn's linear theory of spinodal decomposition predicts for

the time scale $\omega^{-1} \sim (\rho - \rho_{sp}^{-})^{-2}$ of the fastest growing mode when approaching the spinodal density, i.e., a much faster increase than for t.

In Fig. 1(b) we show $U^{-1}(t)$ and $\chi^{-1/2}(t)$, i.e., using the relation (3) the length $L(t)$ as function of time. We observe the scaling behavior $L(t) \sim t^{\alpha}$ with three different scaling exponents α for various hydrodynamic regimes, one with $\alpha = 2/3$ for low viscosities ($\tau = 0.54$, kinetic regime), $\alpha = 1/2$ for intermediate values ($\tau = 0.6$), and $\alpha = 1/3$ for high viscosities ($\tau = 1.5$), which was not reported in Ref. [8] but is well established by the Lifshitz-Slyuzov-Wagner theory [1]. At higher viscosities we do not observe scaling at all at least up to $t \sim 10^6$ time steps. We did several runs and obtained identical behavior, but the data we show in Fig. 1 are obtained after individual runs without any averaging procedure, which is not necessary in order to obtain accurate results. In contrast to Ref. [8], we interpret the scaling regime with $\alpha = 2/3$ not as the late stage, even it is found for low viscosities. It is the same regime where we observe strong oscillations in $F(t)$ and $U(t)$. As long as the fluid velocities are not damped by viscous forces, the kinetic terms in the Navier-Stokes equation are dominant. This is the very early regime established after spinodal decomposition and it can be seen only if it is not damped by viscous forces. These velocities in the beginning of phase seperation have little to do with the velocities during domain growth that are relevant for the exponent $\alpha = 2/3$ at late times. Moreover, we find some evidence that there is a crossover from $\alpha = 2/3$ to $\alpha = 1/2$ as indicated in Fig. 1(b) for $\tau = 0.6$.

We emphasize that the statistical robustness of the morphological measures is essential for the determination of the length L and, in particular, for the determination of the new exponent $\alpha = 1/3$, especially for small system sizes and for the late stage regime, where the number of homogeneous droplets vanish and statistical fluctuations become important. Generally, fluctuations of the morphological measures are small due to the additivity relation (1), in contrast to the domain size calculated from the first zero of the radial distribution function. Since morphological measures show scaling also for large domains at later times, one can extract reliables values for L from these quantities, even in cases where this is not possible by other means.

In conclusion, we made an attempt towards the characterization of the time evolution of the morphology of phase separation. We introduced a method to describe the morphology of patterns and to define the typical length scale. In particular, this method allows us to define the crossover from the early stage decomposition to the late stage growth and to analyze the morphology of decomposition patterns at early times. A comparision of our results with simulations of Ginzburg-Landau models will be done in future work in order to elucidate the differences between conserved and nonconserved order parameters, for instance. We expect the Minkowski functionals to be especially fruitful in three dimensions where the topology of the spatial structure changes considerably with the mean density ρ. The measures may provide a mean to study the dependence of the scaling behavior on the morphology.

V.S. is indebted to Professor Siegfried Dietrich for providing the possibility of a stay in his department and acknowledges also the financial support of the Romanian Ministry of Research and Technology, supervised through the Romanian Space Agency.

[1] J. D. Gunton, M. Miguel, and P. S. Sahni, in *Phase Transition and Critical Phenomena*, edited by C. Domb and J. L. Lebowitz (Academic Press, New York, 1983), Vol. 8; A. J. Bray, Adv. Phys. **43**, 357 (1994).

[2] W. J. Ma, A. Maritan, J. R. Banavar, and J. Koplik, Phys. Rev. A **45**, R5347 (1992); E. Velasco and S. Toxvaerd, Phys. Rev. Lett. **71**, 388 (1993).

[3] E. Velasco and S. Toxvaerd, Phys. Rev. E **54**, 605 (1996).

[4] E. Farrell and O. T. Walls, Phys. Rev. B **40**, 7027 (1989); **42**, 2353 (1990); **43**, 630 (1990); T. Lookman, Y. Wu, F. Alexander, and S. Chen, Phys. Rev. E **53**, 5513 (1996); H. Furukawa, Phys. Rev. A **31**, 1103 (1985); Adv. Phys. **34**, 703 (1985).

[5] D. H. Rothman and J. M. Keller, J. Stat. Phys. **52**, 1119 (1988); C. Appert and S. Zaleski, Phys. Rev. Lett. **64**, 1 (1990); S. Chen, G. D. Doolen, K. Eggert, D. Grunau, and E. Y. Loh, Phys. Rev. A **43**, 7053 (1991).

[6] A. Gunstensen, D. H. Rothman, S. Zaleski, and G. Zannetti, Phys. Rev. A **43**, 4320 (1991); F. J. Alexander, S. Chen, and D. W. Grunau, Phys. Rev. B **48**, 634 (1993).

[7] M. R. Swift, W. R. Osborn, and J. M. Yeomans, Phys. Rev. Lett. **75**, 830 (1995).

[8] W. R. Osborn, E. Orlandini, M. R. Swift, J. M. Yeomans, and J. R. Banavar, Phys. Rev. Lett. **75**, 4031 (1995).

[9] P. V. Coveney and K. Novik, Phys. Rev. E **54**, 5134 (1996).

[10] L. A. Santalò, *Integral Geometry and Geometric Probability* (Addison-Wesley, Reading, MA, 1976).

[11] H. Hadwiger, *Vorlesungen über Inhalt, Oberfläche und Isoperimetrie* (Springer-Verlag, Berlin, 1957).

[12] A. Rosenfeld and A. C. Kak, *Digital Picture Processing* (Academic Press, New York, 1976).

[13] K. R. Mecke, Phys. Rev. E **53**, 4794 (1996).